How to cite: Angew. Chem. Int. Ed. 2024, e202403186
doi.org/10.1002/anie.202403186

Photocatalysis

# CdS Quantum Dot Gels as a Direct Hydrogen Atom Transfer Photocatalyst for C–H Activation

*Daohua Liu, Atanu Hazra, Xiaolong Liu, Rajendra Maity, Ting Tan,* and Long Luo**

**Abstract:** Here, we report CdS quantum dot (QD) gels, a three-dimensional network of interconnected CdS QDs, as a new type of direct hydrogen atom transfer (d-HAT) photocatalyst for C–H activation. We discovered that the photoexcited CdS QD gel could generate various neutral radicals, including α-amido, heterocyclic, acyl, and benzylic radicals, from their corresponding stable molecular substrates, including amides, thio/ethers, aldehydes, and benzylic compounds. Its C–H activation ability imparts a broad substrate and reaction scope. The mechanistic study reveals that this reactivity is intrinsic to CdS materials, and the neutral radical generation did not proceed via the conventional sequential electron transfer and proton transfer pathway. Instead, the C–H bonds are activated by the photoexcited CdS QD gel via a d-HAT mechanism. This d-HAT mechanism is supported by the linear correlation between the logarithm of the C–H bond activation rate constant and the C–H bond dissociation energy (BDE) with a Brønsted slope $\alpha = 0.5$. Our findings expand the currently limited direct hydrogen atom transfer photocatalysis toolbox and provide new possibilities for photocatalytic C–H activation.

## Introduction

Hydrogen atom transfer (HAT) reactions are pivotal in chemical and biochemical processes.[1] In contrast to electron transfer and energy transfer mechanisms, HAT offers a distinctive advantage by overcoming the constraints of redox potentials, thereby activating substrates under mild conditions in organic transformations. HAT in photocatalysis has two approaches: indirect hydrogen atom transfer (i-HAT) and direct hydrogen atom transfer (d-HAT).[1a,2] In the i-HAT process, a photocatalyst is excited upon light absorption to generate radical or radical ion species as hydrogen abstractors through electron transfer events, for example, reduction of persulfate ($S_2O_8^{2-}$) to a sulfate radical anion ($SO_4^{\bullet-}$)[3] and oxidation of thiol (R-SH) to thiyl radical (R-S$^\bullet$).[4] In comparison, the d-HAT process directly abstracts a hydrogen atom from a substrate molecule by an excited photocatalyst, forming a radical intermediate and the H$^\bullet$-doped form of the photocatalyst (PC$^\bullet$-H) (Figure 1a).

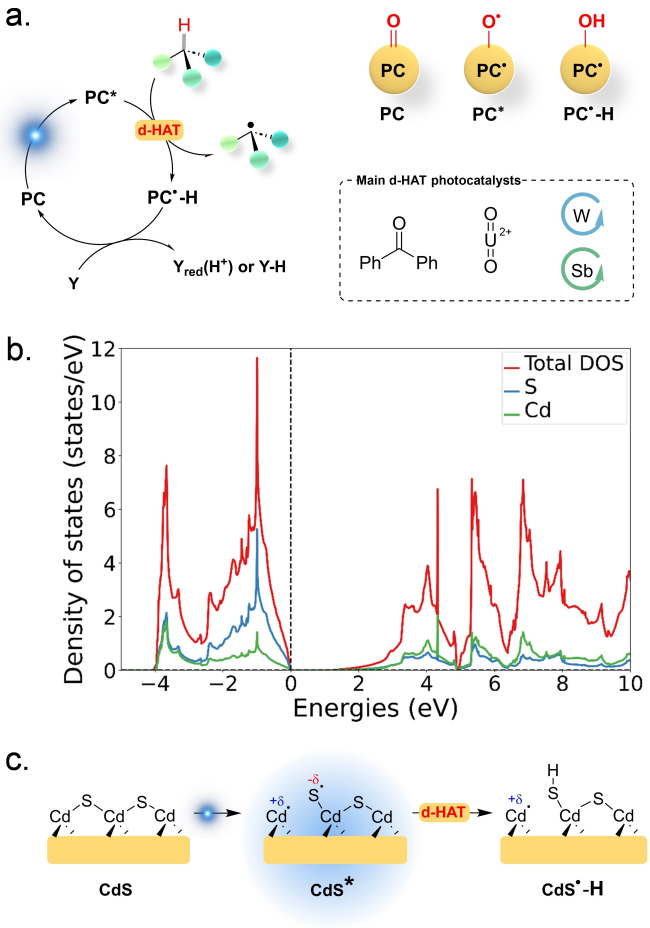


***Figure 1.*** (a) Photocatalyzed d-HAT process and the common d-HAT photocatalysts. (b) Density of state plot for CdS shows the valence band electrons that predominantly reside on the S sites of CdS QDs in the ground state (blue line between 0 and −2 eV), reproduced from the Materials Project database.[5] The dashed line indicates the location of the Fermi level. (c) Proposed d-HAT mechanism for CdS QD gels. The nominal oxidation state of Cd (+δ) in the excited CdS should be between +1 and +2, while that of S (−δ) should be between −2 and −1.

[*] D. Liu, Dr. A. Hazra, Dr. R. Maity, Dr. L. Luo
Department of Chemistry
Wayne State University
5101 Cass Ave, Detroit, MI 48202
E-mail: long.luo@wayne.edu
Dr. X. Liu, Dr. T. Tan
Laboratory of Theoretical and Computational Nanoscience, CAS Center for Excellence in Nanoscience, National Center for Nanoscience and Technology, Chinese Academy of Sciences, Beijing 100190, China
E-mail: tant@nanoctr.cn

The prevalent structural motif in d-HAT photocatalysts features an oxo group, endowing them with a distinctive oxygen-centered radical character in their reactive excited states for hydrogen abstraction. These photocatalysts can be classified as (i) carbonyl derivatives, including aromatic ketones,[6] diacetyls,[7] aldehydes,[8] and neutral Eosin Y,[9] and (ii) inorganic oxide derivatives, including decatungstate anion ($[W_{10}O_{32}]^{4-}$),[10] uranyl cation ($[UO_2]^{2+}$),[11] and antimony oxo porphyrin complexes.[12] However, each d-HAT photocatalyst has its limitations. For example, aromatic ketones could easily undergo irreversible dimerization during photoreaction, and therefore, a high photocatalyst loading (up to a few equivalents relative to substrate) is generally required to compensate for the catalyst loss.[13] Photoexcited $[W_{10}O_{32}]^{4-}$ anion can abstract hydrogen from strong bonds, such as the C–H bond in methane (BDE = 105 kcal mol$^{-1}$).[14] However, its chemistry is mainly restricted by the need for highly energetic UV light (< 400 nm). Therefore, there is still strong interest in discovering new classes of visible-light-absorbing d-HAT photocatalysts that provide bond-cleaving and forming capabilities complementary to the existing ones.

Metal chalcogenide quantum dots (QDs), such as CdS and CdSe, are semiconductor nanocrystals with tunable electronic and optical characteristics by their sizes. Recently, QDs have emerged as powerful photocatalysts in organic synthesis.[15] For example, CdS QDs were found to be a potent photoreductant with a reduction potential < −3.4 V vs SCE due to the Auger process of excited QDs.[16] Moreover, the van der Waals interactions between the CdSe surface and 4-vinylbenzoic acid derivatives enabled regioselective intermolecular [2 + 2] photocycloadditions.[15b,17] In this reaction, up to 98 % switchable regioselectivity and 98 % diastereoselectivity were achieved for the previously minor *syn*-cyclobutane products, including the *syn*-head-to-tail cyclobutane, which has never before been accessed as the major product of a hetero-photocycloaddition using conventional molecular photocatalysts. In addition, Wu et al. recently reported that the CdSe QD surface could also stabilize allylic and thiyl radicals, enabling direct radical cross-coupling for allylic C($sp^3$)-H or vinylic C–H thiolation while releasing $H_2$ as a byproduct.[15h,18] Similar cross-coupling reactions of transient radical intermediates would require a metal co-catalyst using molecular photocatalysts.[19]

CdS QD gels are a 3D connected pore-matter architecture of interconnected CdS QD networks prepared by electrochemical or chemical oxidation of QDs.[20] Compared with colloidal QDs, QD gels lose most surface ligands during gelation but retain the quantum confinement characteristics of the QDs (Figure S1).[20b] Previously, we found that CdS QD gel exhibited higher photocatalytic activity than its ligand-capped CdS QDs with the same band gap because its surface sites are highly accessible to the substrates.[15a] Due to the surface interactions, CdS QD gel also catalyzed a unique ring-opening reaction during α-amine arylation of tetrahydroisoquinoline.

Here, we report CdS QD gels as a new type of d-HAT photocatalyst for activating C–H bonds of a broad range of substrates, including cyclic thio/ethers, amides, aldehydes, and benzylic compounds. The proposed mechanism is that upon photoexcitation, the valence band electrons that predominantly reside on the S sites of CdS QDs in the ground state would partially shift to the Cd sites (Figures 1b and S2). As a result, the excited QDs exhibit the characteristics of thiyl radicals, which are highly reactive toward hydrogen abstractions from C–H bonds (Figure 1c).[21]

## Results and Discussion

### Reaction Development

CdS QD gels were synthesized from trioctylphosphine oxide-capped CdS QDs following a previously reported electrogelation procedure.[20b] Briefly, the trioctylphosphine oxide ligands of QDs were first exchanged with redox-active thioglycolate ligands. Under anodic electrolysis, thiolate ligands are oxidatively removed as disulfides, and CdS QDs are also oxidized to form interparticle dichalcogenide bonds between QDs, forming a three-dimensional QD gel network (Figure S3). The synthesized gel has an average crystallite size of ~3.3 nm, UV/Vis absorption at ~400 nm, band edge emission at ~470 nm, and trap state emission at ~540 nm, like its colloidal QD precursors (Figures S4–6).[15a,22]

To test the photocatalytic C–H bond activation ability of CdS QD gels, we used the alkylation of C–H bonds via radical addition to an electron-deficient alkene (e.g., 2-benzylidene malononitrile **1**) as a model reaction. Initially, we added the C–H partners as the solvent and $2\times10^{-3}$ mol% QD gel catalysts (Method A in Figure 2). The catalyst loading was defined as the molar ratio between QD building units in the added gel catalyst and the limiting reagent (in this case, **1**). The reactions were conducted at room temperature under 440 nm blue light irradiation and Ar atmosphere in the same homebuilt photocatalytic reaction apparatus as our previous work.[15a] Various five-member-ring cyclic ethers, including tetrahydrofuran (THF), 2-methyl-1,3-dioxolane, 1,3-dioxolane, and 2-methyl-tetrahydrofuran afforded their corresponding alkylation products (**3a**–**3d**) in good to excellent yields of 60–96 % in less than 3 hours. However, the six-member ring 1,3-dioxane and 1,4-dioxane only gave a product yield of ~10 %, and the reaction did not complete even after up to 80 hours due to the strong BDE > 90 kcal mol$^{-1}$ (Figure S7). No reaction product was observed without light or QD gel catalyst (Figure S8), confirming the C–H activation was catalyzed by CdS QD gels. DFT calculation was also performed at B3LYP/6-31G(d,p) level with thermal correction at 298 K for the addition reaction with THF. Gibbs free energy change of 0.25 eV indicated the reaction is net-endergonic, and the energy of electromagnetic radiation is partially stored in the products. As a heterogeneous catalyst, CdS QD gel can be easily recycled by centrifugation. The recycled CdS QD gel preserved its mesoporous structure (Figure S9 and S10) and photocatalytic reactivity without appreciable loss in the product yield (Figure S11).

The discovered photocatalytic reaction does not require the C–H partner to be a solvent and can proceed efficiently

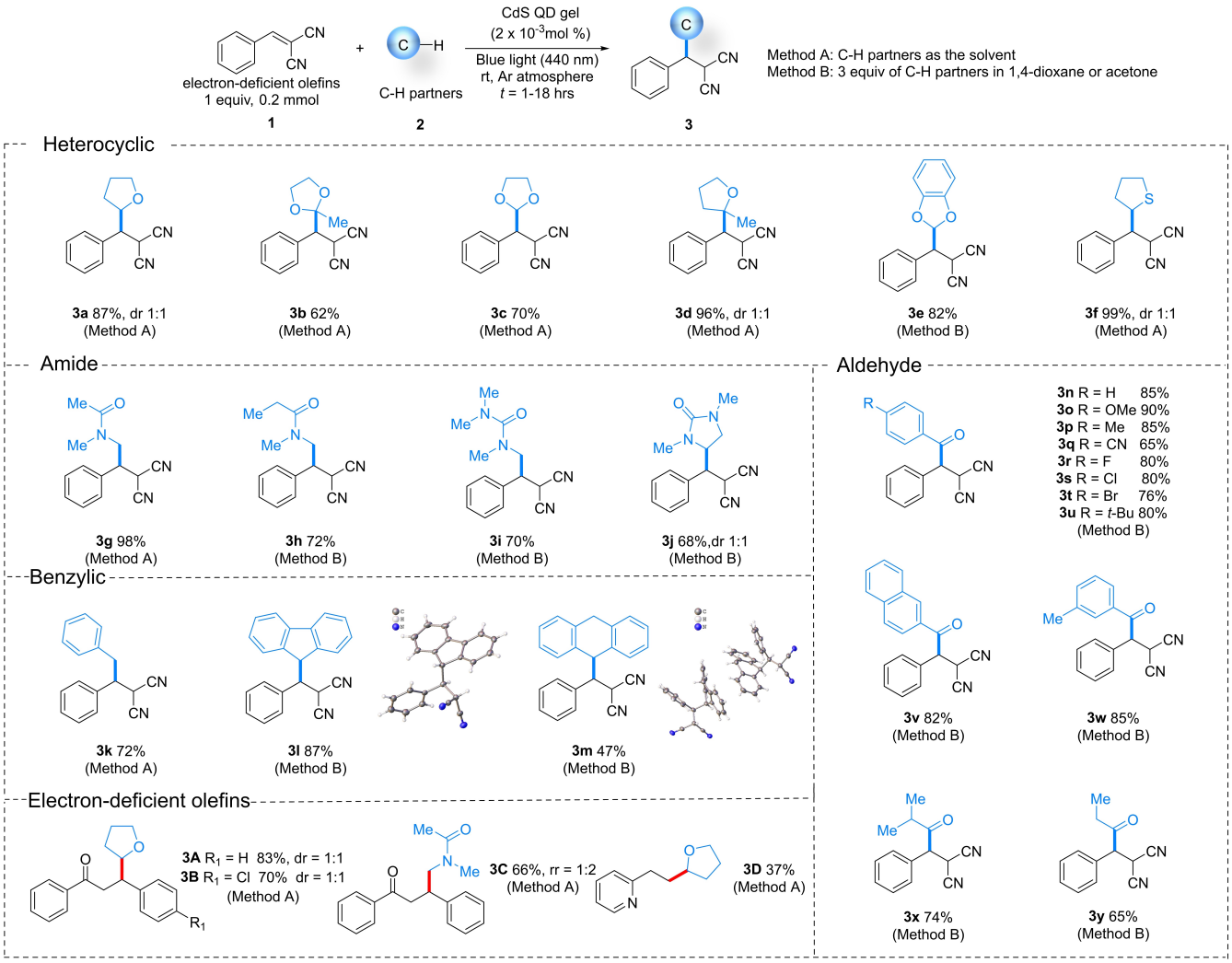


***Figure 2.*** Substrate scopes for the photocatalytic reactions between an electron-deficient alkene **1** and C–H partners **2**. Isolated yields and diastereomeric ratios (dr, determined based on 1H NMR spectra) are shown under each product. rt: room temperature.

with a few equivalents of substrates. For example, 3 equivalents of 1,3-benzodioxole afforded **3e** at an isolated yield of 82 % using 1,4-dioxane as the solvent (Method B in Figure 2). The reaction with tetrahydrothiophene also proceeded smoothly, affording **3f** in an excellent yield of 99 %. Various acyclic (**3g–3i**) and cyclic (**3j**) amide substrates also yielded the corresponding addition products at 70 %–98 % isolated yields using Method A or B. The reaction protocol was easily adapted to activate benzylic C–H bonds, producing **3k**, **3l**, and **3m** at good to excellent yields of 47 % to 87 %. Similar experiments were carried out using other electron-deficient alkenes, including unsaturated ketones such as chalcones (**3A–3C**) and vinyl pyridine (**3D**), resulting in good to excellent yields (37 %–83 %).

In addition to $C(sp^3)$-$C(sp^3)$ bond formation, CdS QD gels also catalyzed $C(sp^2)$-$C(sp^3)$ bond formation using aldehydes as the C–H partner. A broad scope of structurally diverse aldehydes, including aromatic (**3n–3w**) and aliphatic (**3x**, **3y**) ones, were used for the hydroacylation of **1** in good to excellent isolated yields of 60–90 %. We observed faster reactions with aliphatic aldehyde reactions than the aromatic ones (~3 hours vs ~15 hours). This reaction exhibited excellent tolerance towards various functional groups, including halogen, cyano, *t*-butyl, etc.

Besides the addition reactions, we further tested the feasibility of performing photocatalytic radical-radical cross-coupling reactions. We started by exploring the $C(sp^3)$-H bond arylation reaction of amides (Figure 3a). Cyanoaromatics **4** are good electron acceptors for generating aryl radical anions as versatile radical coupling partners through decyanation.[6d,23] The results show that our protocol is compatible with various electron-deficient cyanoaromatics (**6a–6e**) and amides (**6f–6l**), yielding their corresponding arylated products in good to excellent yields of 30 %–96 %. Impressively, all cyclic amides (**6j–6l**) reacted exclusively at their α-*N*-$CH_2$ position, which was not observed in the previous reports on photocatalytic cyclic amide arylation.[24] The reactions using haloaromatics as the coupling partner were unsuccessful, possibly because the aryl radicals generated from haloaromatics are less stable.

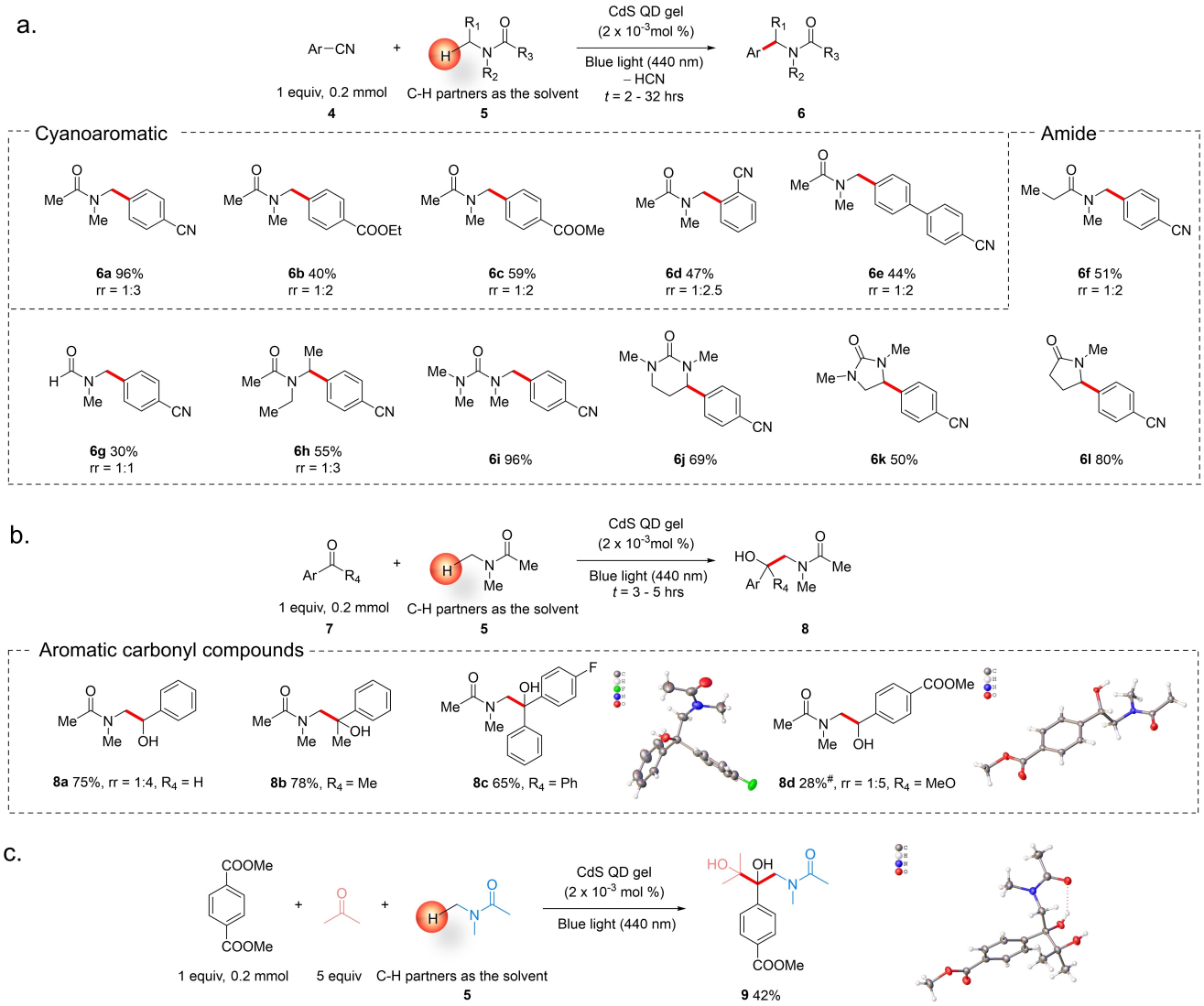


***Figure 3.*** Photocatalytic coupling reactions (a) between amides and cyanoaromatics, (b) between amides and aromatic carbonyl compounds, and (c) three-compound coupling reaction. In all cases, 1 mL C–H partners **5** were used as solvent and $2\times10^{-3}$ mol% CdS QD gel was used as the catalyst. Isolated yields and regioisomeric ratios (rr, calculated from $^{1}$H NMR spectra) are shown under each product. # 6% of ketone product was also obtained (see Figure S6).

Next, we explored the coupling reaction between amide **5** and various aromatic carbonyl compounds **7**, including aldehyde, ketone, and ester (Figure 3b). Attaching photogenerated radical intermediates to C=O bonds is challenging and was achieved only in limited instances, for example, via the reaction between an organochromium-type carbanion species and aldehydes.[10a] Using CdS QD gels as the photocatalyst, we successfully coupled *N*,*N*-dimethylacetamide (DMA) with benzaldehyde (**8a**), acetophenone (**8b**), 4-fluorobenzophenone (**8c**), and dimethyl terephthalate (**8d**) in moderate to excellent yields of 28% to 78%. The reaction between *N*,*N*-dimethylacetamide and dimethyl terephthalate also led to 6% of ketone product (Figure S12). Most impressively, we observed an unusual three-component reaction between *N*,*N*-dimethylacetamide, acetone, and dimethylterephthalate, forming an alkylated pinacol C–C coupling product **9** at a good yield of 42%. The above results have clearly demonstrated that CdS QD gels are a versatile photocatalyst for activating C–H bonds and efficiently utilizing the generated intermediates for coupling reactions.

### *Mechanistic Understanding*

To understand the C–H bond activation mechanism, we started with detecting in situ generated radical intermediates during the photocatalytic reactions. We used 2,2,6,6-tetramethyl-1-piperidinyloxy (TEMPO) as the radical scavenger. We confirmed the formation of α-ethereal, α-amido, acyl, and benzylic radicals from THF, DMA, benzaldehyde, and toluene by detecting their TEMPO adducts using high-resolution mass spectrometry (Figures 4a and S13). Reactions were also completely inhibited due to the presence of

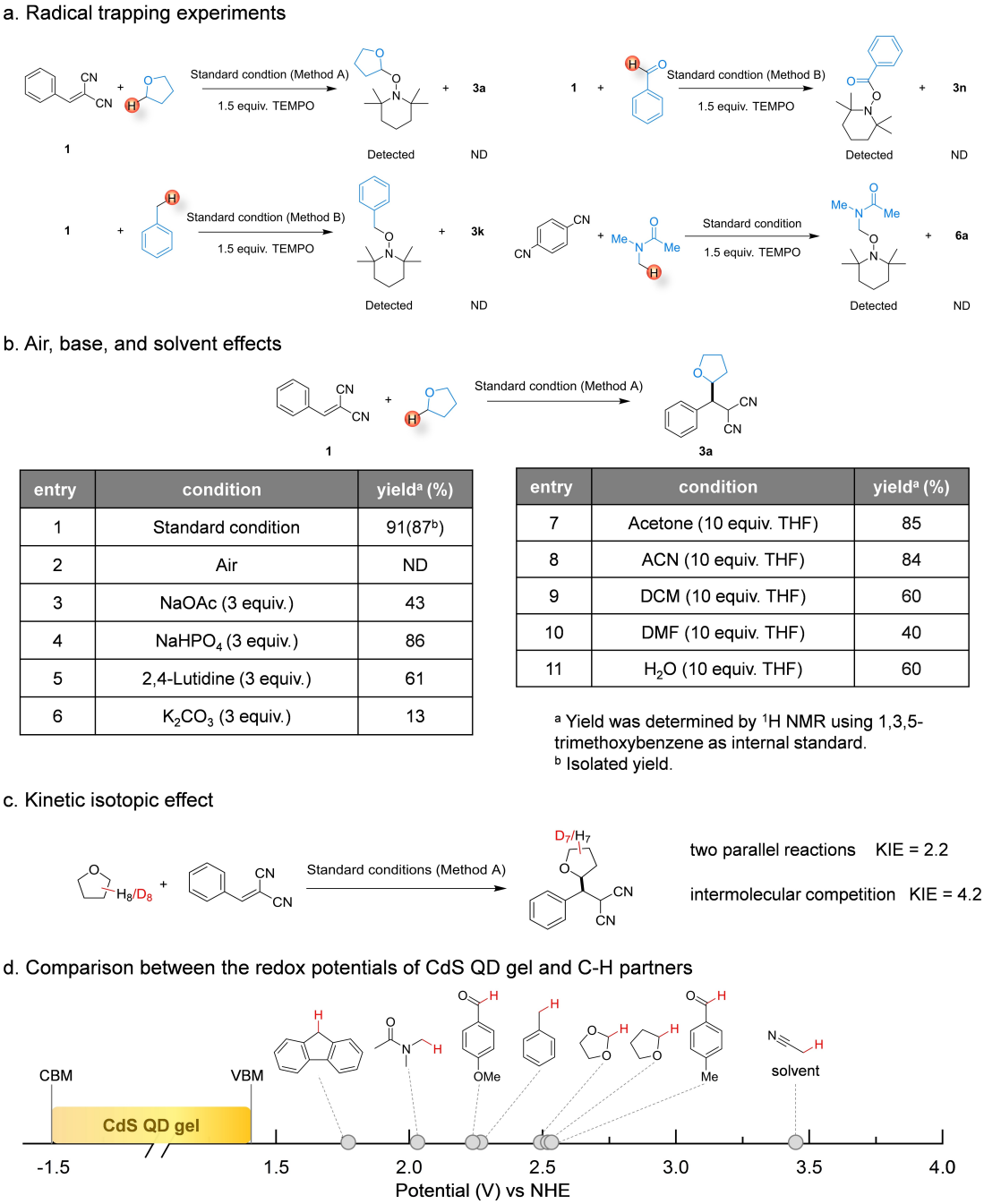


| entry | condition | yield[a] (%) |
|---|---|---|
| 1 | Standard condition | 91(87[b]) |
| 2 | Air | ND |
| 3 | NaOAc (3 equiv.) | 43 |
| 4 | $NaHPO_4$ (3 equiv.) | 86 |
| 5 | 2,4-Lutidine (3 equiv.) | 61 |
| 6 | $K_2CO_3$ (3 equiv.) | 13 |

| entry | condition | yield[a] (%) |
|---|---|---|
| 7 | Acetone (10 equiv. THF) | 85 |
| 8 | ACN (10 equiv. THF) | 84 |
| 9 | DCM (10 equiv. THF) | 60 |
| 10 | DMF (10 equiv. THF) | 40 |
| 11 | $H_2O$ (10 equiv. THF) | 60 |

[a] Yield was determined by $^1H$ NMR using 1,3,5-trimethoxybenzene as internal standard.
[b] Isolated yield.

***Figure 4.*** Mechanism studies. (a) Radical trapping experiments using 2,2,6,6-tetramethyl-1-piperidinyloxy (TEMPO) as the radical scavenger under various coupling reaction conditions. TEMPO adducts were detected by high-resolution mass spectrometry. ND: not detected. (b) Control experiments that evaluated the effect of air, base, and solvent choice. (c) Oxidation potentials of organic substrates, the valence band maximum (VBM) and conduction band minimum (CBM) of CdS QD gel.

TEMPO (Figure 4a). Similar reaction inhibition was observed after exposing the reaction to another common radical scavenger, oxygen molecules (entry 2 in Figure 4b). Both observations indicate that QD gel-catalyzed C–H bond activation led to neutral radical formation. The kinetic isotope effects (KIE) measured from two parallel reactions and intermolecular competition experiment show primary KIE values of 2.2 and 4.2, resulting from H/D substitution of THF (Figures 4c and S14). Similar primary KIE values were observed for C–H activation of amide and benzaldehyde substrates (Figures S15 and S16). These findings indicate that the C–H bond cleavage to form the radical intermediates occurred during the rate-determining step of the photocatalytic reactions.[12,25]

Next, we investigated how these neutral radicals were generated from their corresponding C–H substrates. We initially evaluated the possibility of electron transfer between photoexcited CdS QD gels and substrates, followed

by deprotonation. To test it, we estimated the oxidation potentials of organic substrates from their onset potentials in the cyclic voltammograms (Figure S17). We found that the electrode potentials required to oxidize the organic substrates were significantly higher (by >380 mV) than the valence band maximum (VBM) of CdS QD gel (1.39 V vs NHE,[15a] Figure 4d), indicating the oxidizing power of excited QD gel is insufficient for electron transfer with the C–H substrates. Moreover, control experiments with inorganic or organic bases show that base had no positive effect on THF (entries 3–6 in Figure 4b) or DMA activation (Figures S18–S20), suggesting that deprotonation may not be required for producing these radicals, either. In addition, the photocatalytic reaction is insensitive to solvents (entries 7–11). Similar product yields were observed using acetone, acetonitrile (ACN), dichloromethane (DCM), and even $H_2O$, indicating that carbocation intermediates are unlikely to be present because they would have been attacked by water. The slightly lower yield for dimethylformamide (DMF) is because DMF is also activated under the same reaction conditions (Figure 3a).

The wide range of possible C–H bonds to be activated, along with the inefficient oxidizing power of CdS QD gels, the absence of the need for bases, and the insensitivity to solvents all suggest that there might be an alternative mechanism for C–H bond activation that differs from the sequential electron transfer and proton transfer pathway.

We also ruled out the possibility of an i-HAT pathway via thiyl radicals from the oxidation of thiol ligands that were possibly not fully removed during QD gel synthesis. The reasons are two-fold. First, adding thiol suppressed the C–H activation; and second, commercial CdS powder without any thiol ligands exhibited similar C–H activation capability, albeit less efficient than CdS QD gel (entries 2 and 5 in Figure S21). These findings indicate that CdS material has an inherent ability to activate C–H bonds photocatalytically, regardless of their form. In addition, we investigated the possibility of energy transfer processes operative in our reaction by adding anthracene, a triplet energy quencher (Figure S22). We still obtained a 57% yield, suggesting that energy transfer processes do not play a major role in the reaction. Inspired by the similarity between metal oxides and metal sulfides, we hypothesized that the CdS QD gels activate the C–H bonds through a d-HAT mechanism. This mechanism involves excited QD gels exhibiting the characteristics of thiyl radicals, which allows them to abstract hydrogen from C–H bonds.

### *Correlation Between Reaction Kinetics and Bond Dissociation Enthalpies*

To test this hypothesis, we studied the correlation between reaction kinetics and C–H BDEs. According to the Evans-Polanyi model, the log of rate constants should parallel the reaction energy within a set of atom transfer reactions, including many HAT reactions.[25c,26] The differences in reaction energies are usually taken as the differences in the C–H BDEs.[27] In our case, the d-HAT reaction involving photoexcited CdS QD gel reacting with various C–H substrates should also follow this rate/C–H BDE correlation.

We chose the α-ethereal radical addition to **1** as a model reaction (Figure 5a). As previously discussed in Figure 4c, the C–H bond activation of cyclic ether is the rate-determining step of this reaction so the overall reaction rate ($v$) can be expressed as $v = k_{\text{d-HAT}}$ [C–H] [CdS*] (eq 1), where $k_{\text{d-HAT}}$ is the rate constant of the d-HAT process, [C–H] is the concentration of cyclic ether substrate, and [CdS*] is the concentration of reactive surface sites in excited CdS QD gel. However, it is challenging to measure $k_{\text{d-HAT}}$ because of the difficulty in accurately quantifying [CdS*]. Considering that [CdS*] should roughly remain the same under a fixed light intensity and QD gel loading, we could still establish the correlation between reaction kinetics and C–H BDE from the measured pseudo-first-order rate constant $k_{\text{obs}} = k_{\text{d-HAT}}$[CdS*].

The $k_{\text{obs}}$ values were measured under a modified reaction condition where cyclic ether is the limiting reagent, as shown in Figure 5b. Figure 5c shows the percentage change of [C–H] ([C–H]/[C–H]$_0$) as a function of reaction time for methyl 1,3-dioxolane. [C–H] was monitored using $^1$H NMR (Figure S23). The plot of ln([C–H]/[C–H]$_0$) vs. reaction time shows a linear relationship over 9 hours, indicating a pseudo-first-order reaction mechanism. $k_{\text{obs}}$ is measured to be $4.2\times10^{-5}$ s$^{-1}$ from the slope of the linear fit. The change of [**1**] and [C–H]$_0$ did not alter $k_{\text{obs}}$, but reduced catalyst loading by 50% decreased $k_{\text{obs}}$, by ~50%. In addition, the lowered light intensity also lowered $k_{\text{obs}}$. All of the above observations are consistent with the reaction rate model in Figure 5a, where $k_{\text{obs}}$ is proportional to [CdS*] but independent on [**1**] or [C–H]$_0$.

Similar measurements of $k_{\text{obs}}$ were conducted for cyclic ethers with different C–H BDEs. All the reactions exhibited pseudo-first-order kinetics at the initial stage of ~4 hours (Figures S23–S36). The measured $k_{\text{obs}}$ was normalized by the number of abstractable C–H bonds of cyclic ethers, for example, 4 for THF and 1 for methyl 1,3-dioxolane.[28] The plot of log(normalized $k_{obs}$) and calculated C–H BDEs exhibited a good linear correlation, giving a Brønsted slope $\alpha = 0.5$ (Figure 4e). A value of α close to 0.5 is predicted by most rate/driving force relations for reactions with a transition state near the midpoint of the reaction coordinate,[29] including sets of similar HAT reactions with small reaction free energy changes.[27,30] This finding confirms that the CdS QD gel activates C–H bonds via a d-HAT mechanism.

### *Observation of CdS•-H Formation*

According to our proposed mechanism in Figure 5a, CdS QD gel should form the H•-doped CdS (CdS•-H) after abstracting a hydrogen atom from C–H substrates during d-HAT.[31] To observe the formation of CdS•-H, we mixed CdS QD gel with a stable aprotic C–H partner, toluene, under water- and air-free conditions. After blue light irradiation for 10 mins, we observed a color change of the

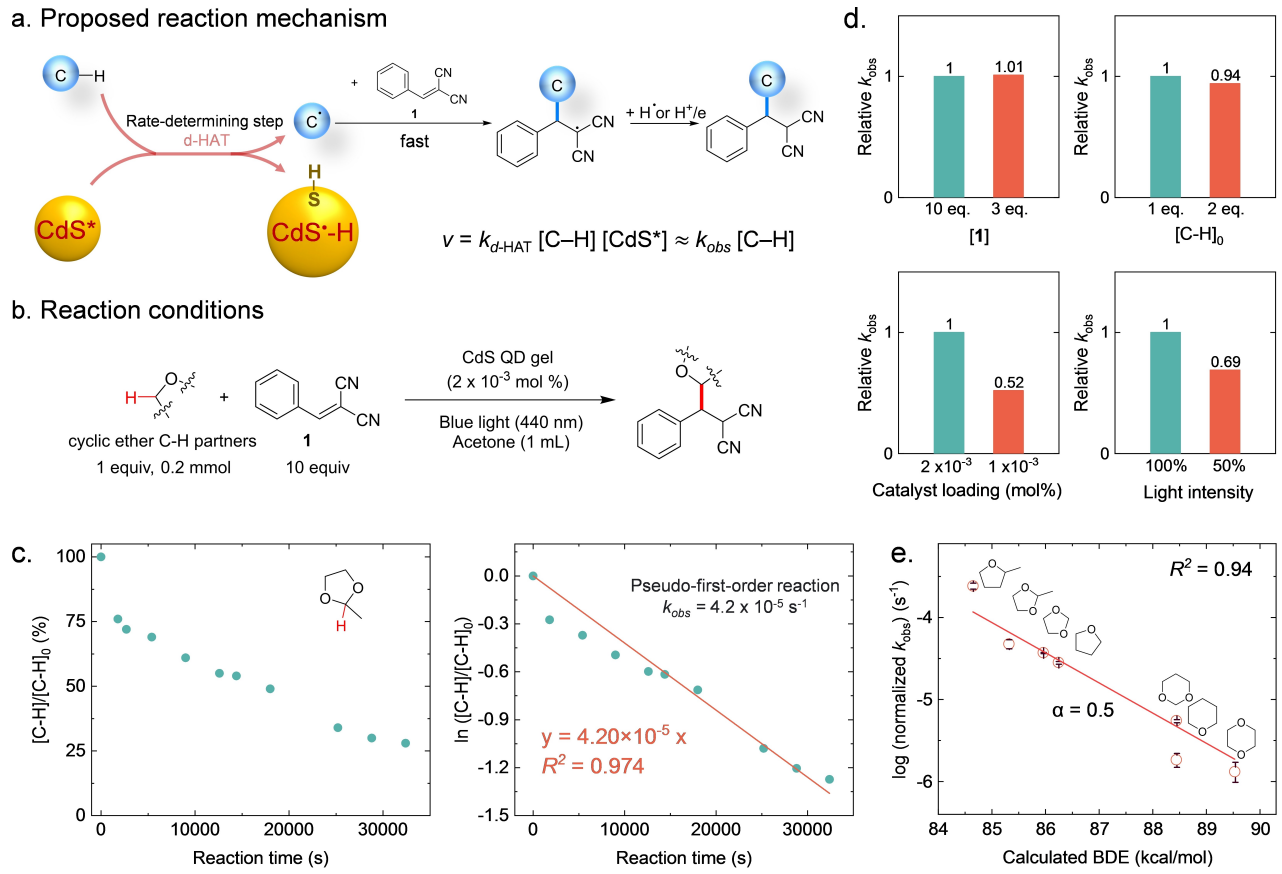


***Figure 5.*** Reaction kinetics study. (a) Proposed mechanism for the photocatalytic addition reaction between C–H substrates and **1** using CdS QD gel catalyst. Inset: the reaction rate expression. (b) Reaction conditions for kinetics studies using cyclic ethers as the C–H partners. (c) Time-dependent plots of $[C–H]/[C–H]_0$ and $\ln([C–H]/[C–H]_0)$ during the photocatalytic reaction of methyl 1,3-dioxolane with **1**. (d) Relative $k_{obs}$ under different **1** and methyl 1,3-dioxolane concentrations ([**1**] and $[C–H]_0$), catalyst loadings, and light intensities. (e) Plot of measured normalized $k_{obs}$ vs calculated C–H BDEs. $k_{obs}$ is normalized by the number of abstractable C–H bonds of cyclic ethers. $\alpha$ is the Brønsted slope obtained from the linear fit of the plot.

reaction mixture from yellow (CdS QD gel's original color) to brown (Figures 6b and S37). The brown hue returned to yellow after exposing the solution to air (Figure 6c). Similar reversible color changes were also previously observed when $TiO_2$ and ZnO nanoparticles were irradiated by UV light and then exposed to oxidants such as TEMPO and air.[32] The altered color was attributed to the formation and consumption of the protonated reduced $TiO_2$ and ZnO nanoparticles ($H^+$-$TiO_2$/$e^-$ and $H^+$-ZnO/$e^-$). Note, $H^+$/e is equivalent to a hydrogen atom ($H^•$), so $H^+$-$TiO_2$/$e^-$ and $H^+$-ZnO/e can be considered as $H^•$-doped $TiO_2$ and ZnO.[32] Also, the observed brown color in Figure 6b is similar to the color of reduced CdS QDs prepared by chemical reduction using Na/biphenyl or photochemical reduction in the presence of reductants such as alkyl amines.[16,33] The above evidence supports that $CdS^•$-H was formed from CdS QD gel during the d-HAT process. However, we want to point out that the $H^•$-doped photocatalysts in the previous studies were formed via an electron transfer process, but, in our case, it should result from the d-HAT process between excited CdS QD gel and C–H substrates.

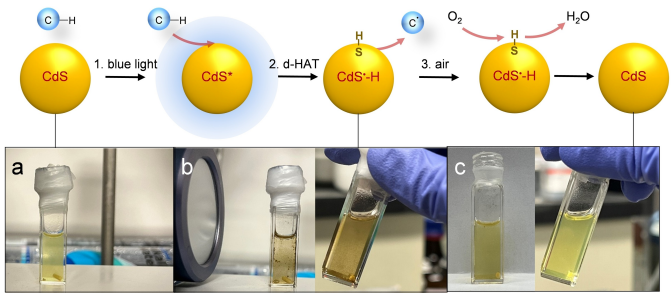


***Figure 6.*** Observation of $CdS^•$-H formation. Photographs of (a) dispersed CdS QD gel in water- and air-free toluene, (b) after blue light irradiation, and (c) after exposure to air.

## *Conclusions*

In this work, we have demonstrated CdS QD gels as a capable d-HAT photocatalyst to activate C–H bonds in various substrates, including cyclic ethers, amides, aldehydes, and benzylic compounds, to generate α-ethereal, α-

amido, acyl, and benzylic radicals and enable versatile radical-based coupling reactions. The redox potential mismatch between the excited QD gel and C–H substrates, solvent, and base insensitivity suggests that C–H bond activation is unlikely to proceed via a sequential electron transfer and proton transfer pathway. The linear correlation between the log of rate constants and the C–H BDEs with a Brønsted slope $\alpha = 0.5$ indicates that C–H bond activation should proceed via a d-HAT mechanism, in which photoexcited CdS QD gels directly attract a hydrogen atom from the C–H substrate. The H•-doped CdS (CdS•-H) formed after H atom abstraction during the d-HAT process was also observed. The discovery of CdS as a new group of d-HAT catalysts will enrich the currently limited d-HAT catalysis toolbox and provide unique bond-cleaving and forming capabilities for organic transformations. Currently, our protocol only efficiently activates $C(sp^3)$-H bonds with BDE values $< 90$ kcal mol$^{-1}$, limited by its visible light absorption at 440 nm wavelength. However, this limitation can be overcome by tuning the band gap of QD gel via its physical size, utilizing its quantum confinement properties. In addition, our discovery of the unique d-HAT behavior of CdS materials arises from the oxidative gelation process that removes the surface ligands. A similar strategy can be applied to other semiconductor materials, such as $MoS_2$, to explore their surface-specific photocatalytic properties.

## Supporting Information

Detailed experimental procedures, theoretical calculation and results, photographs of the experimental setup, TEM, and UV/Vis spectroscopic data, HRMS spectra, recyclability data, kinetic isotope effect study, CV data, NMR spectra, base investigation, $^1$H NMR selectivity monitor time-dependent result, and X-ray crystallographic data and structure refinement.

CCDC 2331306, 2331309, 2331310, 2331312, and 2331313 are available free of charge via the Internet contains the supplementary crystallographic data for this paper. These data can be obtained free of charge via www.ccdc.cam.ac.uk/data request/cif, or by emailing data request@ccdc.cam.ac.uk, or by contacting The Cambridge Crystallographic Data Centre, 12 Union Road, Cambridge CB2 1EZ, UK; fax: +44 1223 336033.

## Acknowledgements

This work was primarily supported by NSF CHE-2247057 to L.L. The preliminary study was supported by NIH 1R35GM142590 to L.L., and the substrate and reaction scope development was partially supported by the NSF Center for Synthetic Organic Electrochemistry, CHE-2002158 to L.L. D.L. acknowledges the support from the Thomas C. Rumble University Graduate Fellowship from Wayne State University. This work made use of the single-crystal XRD that is funded by the NIH supplement grant #3R01EB027103-02S1, NMR data supported by NIH S10OD028488, GC/MS and HRMS analysis is supported by NIH R01 GM098285-07S, the Talos F200X G2 S/TEM analysis is funded in part through NSF MRI award #2018587.

## Conflict of Interest

The authors declare no conflict of interest.

## Data Availability Statement

The data that support the findings of this study are available in the supplementary material of this article.

**Keywords:** Photocatalysis · Quantum dots · Direct hydrogen atom transfer · Heterogeneous catalysis · Radical reactions

[1] a) L. Capaldo, D. Ravelli, M. Fagnoni, *Chem. Rev.* **2021**, *122*, 1875–1924; b) J. Rui, Q. Zhao, A. J. Huls, J. Soler, J. C. Paris, Z. Chen, V. Reshetnikov, Y. Yang, Y. Guo, M. Garcia-Borràs, *Science* **2022**, *376*, 869–874.
[2] H. Cao, X. Tang, H. Tang, Y. Yuan, J. Wu, *Chem Catalysis* **2021**, *1*, 523–598.
[3] J. Jin, D. W. MacMillan, *Angew. Chem.* **2015**, *127*, 1585–1589.
[4] a) Q.-Y. Meng, T. E. Schirmer, A. L. Berger, K. Donabauer, B. König, *J. Am. Chem. Soc.* **2019**, *141*, 11393–11397; b) J. Jin, D. W. C. MacMillan, *Nature* **2015**, *525*, 87–90.
[5] A. Jain, S. P. Ong, G. Hautier, W. Chen, W. D. Richards, S. Dacek, S. Cholia, D. Gunter, D. Skinner, G. Ceder, *APL Mater.* **2013**, *1*.
[6] a) B. Fraser-Reid, N. Holder, M. Yunker, *J. Chem. Soc. Chem. Commun.* **1972**, 1286–1287; b) D. Dondi, S. Protti, A. Albini, S. M. Carpio, M. Fagnoni, *Green Chem.* **2009**, *11*, 1653–1659; c) J.-B. Xia, C. Zhu, C. Chen, *J. Am. Chem. Soc.* **2013**, *135*, 17494–17500; d) T. Hoshikawa, M. Inoue, *Chem. Sci.* **2013**, *4*, 3118–3123; e) S. Kamijo, M. Hirota, K. Tao, M. Watanabe, T. Murafuji, *Tetrahedron Lett.* **2014**, *55*, 5551–5554; f) S. Kamijo, G. Takao, K. Kamijo, M. Hirota, K. Tao, T. Murafuji, *Angew. Chem. Int. Ed.* **2016**, *55*, 9695–9699; g) E. E. Stache, V. Kottisch, B. P. Fors, *J. Am. Chem. Soc.* **2020**, *142*, 4581–4585.
[7] C.-Y. Huang, J. Li, W. Liu, C.-J. Li, *Chem. Sci.* **2019**, *10*, 5018–5024.
[8] M. Fagnoni, S. Protti, D. Ravelli, *Photoorganocatalysis in organic synthesis, Vol. 18*, World Scientific, **2019**.
[9] a) X. Z. Fan, J. W. Rong, H. L. Wu, Q. Zhou, H. P. Deng, J. D. Tan, C. W. Xue, L. Z. Wu, H. R. Tao, J. Wu, *Angew. Chem.* **2018**, *130*, 8650–8654; b) X. Fan, P. Xiao, Z. Jiao, T. Yang, X. Dai, W. Xu, J. D. Tan, G. Cui, H. Su, W. Fang, J. Wu, *Angew. Chem. Int. Ed.* **2019**, *58*, 12580–12584; c) J. Yan, H. W. Cheo, W. K. Teo, X. Shi, H. Wu, S. B. Idres, L.-W. Deng, J. Wu, *J. Am. Chem. Soc.* **2020**, *142*, 11357–11362.
[10] a) K. Yahata, S. Sakurai, S. Hori, S. Yoshioka, Y. Kaneko, K. Hasegawa, S. Akai, *Org. Lett.* **2020**, *22*, 1199–1203; b) V. D. Waele, O. Poizat, M. Fagnoni, A. Bagno, D. Ravelli, *ACS Catal.* **2016**, *6*, 7174–7182; c) D. Ravelli, M. Fagnoni, T. Fukuyama, T. Nishikawa, I. Ryu, *ACS Catal.* **2018**, *8*, 701–713; d) H. Qrareya, D. Dondi, D. Ravelli, M. Fagnoni, *ChemCatChem* **2015**, *7*, 3350–3357; e) G. Laudadio, S. Govaerts, Y. Wang, D. Ravelli, H. F. Koolman, M. Fagnoni, S. W. Djuric, T. Noël, *Angew. Chem. Int. Ed.* **2018**, *57*, 4078–4082.

[11] a) L. Capaldo, D. Merli, M. Fagnoni, D. Ravelli, *ACS Catal.* **2019**, *9*, 3054–3058; b) J. G. West, T. A. Bedell, E. J. Sorensen, *Angew. Chem. Int. Ed.* **2016**, *55*, 8923–8927.
[12] L. Capaldo, M. Ertl, M. Fagnoni, G. Knör, D. Ravelli, *ACS Catal.* **2020**, *10*, 9057–9064.
[13] A. M. Cardarelli, M. Fagnoni, M. Mella, A. Albini, *J. Org. Chem.* **2001**, *66*, 7320–7327.
[14] a) C. B. Musgrave III, K. Olsen, N. S. Liebov, J. T. Groves, W. A. Goddard III, T. B. Gunnoe, *ACS Catal.* **2023**, *13*, 6382–6395; b) G. Laudadio, Y. Deng, K. van der Wal, D. Ravelli, M. Nuño, M. Fagnoni, D. Guthrie, Y. Sun, T. Noël, *Science* **2020**, *369*, 92–96.
[15] a) D. Liu, J. Nyakuchena, R. Maity, X. Geng, J. P. Mahajan, C. C. Hewa-Rahinduwage, Y. Peng, J. Huang, L. Luo, *Chem. Commun.* **2022**, *58*, 11260–11263; b) Y. S. Jiang, C. Wang, C. R. Rogers, M. S. Kodaimati, E. A. Weiss, *Nat. Chem.* **2019**, *11*, 1034–1040; c) J. A. Caputo, L. C. Frenette, N. Zhao, K. L. Sowers, T. D. Krauss, D. J. Weix, *J. Am. Chem. Soc.* **2017**, *139*, 4250–4253; d) X. J. Wu, S. J. Xie, C. X. Liu, C. Zhou, J. C. Lin, J. C. Kang, Q. H. Zhang, Z. H. Wang, Y. Wang, *ACS Catal.* **2019**, *9*, 8443–8451; e) S. C. Jensen, S. B. Homan, E. A. Weiss, *J. Am. Chem. Soc.* **2016**, *138*, 1591–1600; f) M. Y. Qi, Y. H. Li, M. Anpo, Z. R. Tang, Y. J. Xu, *ACS Catal.* **2020**, *10*, 14327–14335; g) L. Korala, J. R. Germain, E. Chen, I. R. Pala, D. Li, S. L. Brock, *Inorg. Chem. Front.* **2017**, *4*, 1451–1457; h) C. Huang, R.-N. Ci, J. Qiao, X.-Z. Wang, K. Feng, B. Chen, C.-H. Tung, L.-Z. Wu, *Angew. Chem. Int. Ed.* **2021**, *60*, 11779–11783.
[16] J. K. Widness, D. G. Enny, K. S. McFarlane-Connelly, M. T. Miedenbauer, T. D. Krauss, D. J. Weix, *J. Am. Chem. Soc.* **2022**, *144*, 12229–12246.
[17] a) Y. Jiang, R. López-Arteaga, E. A. Weiss, *J. Am. Chem. Soc.* **2022**, *144*, 3782–3786; b) C. T. Eckdahl, C. Ou, S. Padgaonkar, M. C. Hersam, E. A. Weiss, J. A. Kalow, *Org. Biomol. Chem.* **2022**, *20*, 6201–6210.
[18] a) C. Huang, J. Qiao, R.-N. Ci, X.-Z. Wang, Y. Wang, J.-H. Wang, B. Chen, C.-H. Tung, L.-Z. Wu, *Chem* **2021**, *7*, 1244–1257; b) L.-M. Zhao, Q.-Y. Meng, X.-B. Fan, C. Ye, X.-B. Li, B. Chen, V. Ramamurthy, C.-H. Tung, L.-Z. Wu, *Angew. Chem. Int. Ed.* **2017**, *56*, 3020–3024.
[19] a) Y. Qin, R. Sun, N. P. Gianoulis, D. G. Nocera, *J. Am. Chem. Soc.* **2021**, *143*, 2005–2015; b) J. C. Tellis, C. B. Kelly, D. N. Primer, M. Jouffroy, N. R. Patel, G. A. Molander, *Acc. Chem. Res.* **2016**, *49*, 1429–1439.
[20] a) C. C. Hewa-Rahinduwage, K. L. Silva, S. L. Brock, L. Luo, *Chem. Mater.* **2021**, *33*, 4522–4528; b) C. C. Hewa-Rahinduwage, X. Geng, K. L. Silva, X. Niu, L. Zhang, S. L. Brock, L. Luo, *J. Am. Chem. Soc.* **2020**, *142*, 12207–12215; c) I. U. Arachchige, S. L. Brock, *J. Am. Chem. Soc.* **2006**, *128*, 7964–7971; d) J. L. Mohanan, I. U. Arachchige, S. L. Brock, *Science* **2005**, *307*, 397–400; e) X. Geng, D. Liu, C. C. Hewa-Rahinduwage, S. L. Brock, L. Luo, *Acc. Chem. Res.* **2023**, *56*, 1087–1096.
[21] F. Dénès, M. Pichowicz, G. Povie, P. Renaud, *Chem. Rev.* **2014**, *114*, 2587–2693.
[22] S. Aryal, J. Frimpong, Z.-F. Liu, *J. Phys. Chem. Lett.* **2022**, *13*, 10153–10161.
[23] a) A. McNally, C. K. Prier, D. W. MacMillan, *Science* **2011**, *334*, 1114–1117; b) S. Tong, K. Li, X. Ouyang, R. Song, J. Li, *Green Synthesis and Catalysis* **2021**, *2*, 145–155; c) M. T. Pirnot, D. A. Rankic, D. B. C. Martin, D. W. C. MacMillan, *Science* **2013**, *339*, 1593–1596; d) K. Qvortrup, D. A. Rankic, D. W. C. MacMillan, *J. Am. Chem. Soc.* **2014**, *136*, 626–629; e) J. D. Cuthbertson, D. W. C. MacMillan, *Nature* **2015**, *519*, 74.
[24] a) S. Das, K. Murugesan, G. J. Villegas Rodríguez, J. Kaur, J. P. Barham, A. Savateev, M. Antonietti, B. König, *ACS Catal.* **2021**, *11*, 1593–1603; b) C. Dai, F. Meschini, J. M. R. Narayanam, C. R. J. Stephenson, *J. Org. Chem.* **2012**, *77*, 4425–4431; c) R. Ueno, E. Shirakawa, *Org. Biomol. Chem.* **2014**, *12*, 7469–7473; d) Y.-Y. Gui, X.-W. Chen, W.-J. Zhou, D.-G. Yu, *Synlett* **2017**, *28*, 2581–2586; e) J. Kaur, A. Shahin, J. P. Barham, *Org. Lett.* **2021**, *23*, 2002–2006.
[25] a) F. Westheimer, *Chem. Rev.* **1961**, *61*, 265–273; b) E. M. Simmons, J. F. Hartwig, *Angew. Chem. Int. Ed.* **2012**, *51*, 3066–3072; c) X.-S. Xue, P. Ji, B. Zhou, J.-P. Cheng, *Chem. Rev.* **2017**, *117*, 8622–8648.
[26] a) M. G. Evans, M. Polanyi, *Trans. Faraday Soc.* **1938**, *34*, 11–24; b) M. Salamone, M. Galeotti, E. Romero-Montalvo, J. v. Santen, B. Groff, J. M. Mayer, G. DiLabio, M. Bietti, *J. Am. Chem. Soc.* **2021**, *143*, 11759–11776.
[27] J. M. Mayer, *Acc. Chem. Res.* **2011**, *44*, 36–46.
[28] I. Ghosh, S. Banerjee, S. Paul, T. Corona, T. K. Paine, *Angew. Chem.* **2019**, *131*, 12664–12669.
[29] S. S. Shaik, H. B. Schlegel, S. Wolfe, *Theoretical Aspects of Physical Organic Chemistry: The SNSUB 2/SUB Mechanism*, Wiley, **1992**.
[30] T. Matsuo, J. M. Mayer, *Inorg. Chem.* **2005**, *44*, 2150–2158.
[31] J. M. Mayer, *J. Am. Chem. Soc.* **2023**, *145*, 7050–7064.
[32] J. N. Schrauben, R. Hayoun, C. N. Valdez, M. Braten, L. Fridley, J. M. Mayer, *Science* **2012**, *336*, 1298–1301.
[33] a) K. E. Shulenberger, H. R. Keller, L. M. Pellows, N. L. Brown, G. Dukovic, *J. Phys. Chem. C* **2021**, *125*, 22650–22659; b) M. Shim, P. Guyot-Sionnest, *Nature* **2000**, *407*, 981–983.

Manuscript received: February 14, 2024
Accepted manuscript online: June 20, 2024
Version of record online: ■■, ■■

# Research Article

*Photocatalysis*

D. Liu, A. Hazra, X. Liu, R. Maity, T. Tan,* L. Luo* **e202403186**

CdS Quantum Dot Gels as a Direct Hydrogen Atom Transfer Photocatalyst for C–H Activation

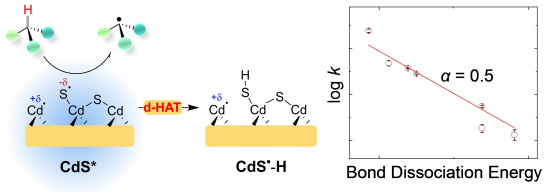


CdS quantum dot gels are potent direct hydrogen atom transfer (d-HAT) photocatalysts for C–H bond activation, in which photoexcited CdS directly attracts a hydrogen atom from a C–H substrate to generate a neutral radical.